BIOCHEMISTRY
including biophysical chemistry & molecular biology

Article

pubs.acs.org/biochemistry

Copper(II) Sequentially Loads onto the N-Terminal Amino Group of the Cellular Prion Protein before the Individual Octarepeats

Helen F. Stanyon, Khushbu Patel, Nadia Begum, and John H. Viles*

School of Biological and Chemical Sciences, Queen Mary, University of London, Mile End Road, London E1 4NS, U.K.

Supporting Information

ABSTRACT: The cellular prion protein (PrP^C) binds to Cu^{2+} ions *in vivo*, and a misfolded form of PrP^C is responsible for a range of transmissible spongiform encephalopathies. Recently, disruption of Cu^{2+} homeostasis in mice has been shown to impart resistance to scrapie infection. Using full-length PrP^C and model peptide fragments, we monitor the sequential loading of Cu^{2+} ions onto PrP^C using visible circular dichroism. We show the N-terminal amino group of PrP^C is not the principal binding site for Cu^{2+}; however, surprisingly, it has an affinity for Cu^{2+} tighter than that of the individual octarepeat binding sites present within PrP^C. We re-evaluate what is understood about the sequential loading of Cu^{2+} onto the full-length protein and show for the first time that Cu^{2+} loads onto the N-terminal amino group before the single octarepeat binding sites.

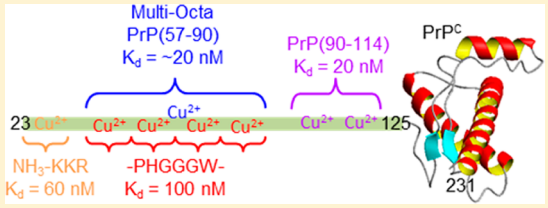

There is intense interest in Cu^{2+} and other metal ions binding to amyloidogenic proteins, in particular amyloid-β peptide (Aβ) in Alzheimer's disease, α-synuclein (αSyn) in Parkinson's disease, and the prion protein (PrP) in transmissible spongiform encephalopathies (TSEs).[1,2] Cu^{2+} ions bind to PrP^C *in vivo*[3] and induce PrP^C endocytosis,[4] while PrP^C mediates Zn^{2+} ion uptake.[5] Recently, it has been shown that transgenic mice with a Menkes disease (Atp7a) mutation are resistant to scrapie infection, creating a strong link between copper homeostasis and prion disease.[6] Furthermore, prion-related scrapie isolates have been found to contain Cu^{2+} ions.[7] Moreover, copper chelation has been shown to delay the onset of prion disease in mice.[8] Interestingly, binding of Cu^{2+} to PrP^C has also been linked to Aβ toxicity in Alzheimer's disease.[9,10] It is for these reasons that much effort has been directed at characterizing the coordination and affinity of binding of Cu^{2+} to PrP^C (for reviews, see refs 1, 11, and 12). As many as six Cu^{2+} ions have been shown to coordinate to the natively unstructured N-terminal domain of PrP^C,[13] with two binding sites in the amyloidogenic region anchored at His^{111} and His^{96}, and up to four binding sites anchored at the four His residues within the octarepeat region. Visible circular dichroism (Vis-CD) has proven to be quite a powerful approach to study Cu^{2+} coordination with broadly four different types of Cu^{2+} coordination described, which generate very different Vis-CD spectra.[12−18]

The locus of binding of Cu^{2+} to both αSyn and Aβ has been shown to directly involve coordination at the N-terminal amino group.[19,20] In contrast, Cu^{2+} binding via the N-terminal amino group of PrP^C has not previously been highlighted.[11,13] We therefore wanted to probe Cu^{2+} coordination and affinity directly at the N-terminal amino group of PrP^C. Here we use Vis-CD to directly monitor Cu^{2+} binding affinity using glycine as a competitive ligand and compare binding of Cu^{2+} to model peptides at the N-terminus to binding of Cu^{2+} to full-length PrP^C.

MATERIALS AND METHODS

Peptides. Fmoc chemistry was used to synthesize the various peptides used. All peptides were C-terminally amidated to mimic the continuation of the peptide sequence in the larger protein. The peptides were removed from the resin and deprotected before being purified by reverse-phase high-performance liquid chromatography. The samples were characterized using mass spectrometry and ^1H nuclear magnetic resonance spectroscopy. Peptides with amidated C-termini and free N-terminal amino groups studied included KKR, MKK, and AAA. The single-octarepeat peptide and PrP(58−91) were acetylated at their N-termini in addition to amidation at their C-termini (sequences of GQPHGGGWGQP and GQPHGG-GWGQPHGGGWGQPHGGGWGQPHGGGWGQP, respectively) [purchased from Generon Ltd. (Maidenhead, U.K.)].

Circular Dichroism (CD). Typically, CD spectra were recorded at 25 °C on an Applied Photophysics Chirascan instrument between 260 and 800 nm, with sampling points every 2 nm, using a 1 cm path-length cell. Three scans were recorded, and baseline spectra were subtracted from each spectrum followed by smoothing using a window of 6 nm. Data were processed using an Applied Photophysics Chirascan Viewer, Microsoft Excel, and the KaleidaGraph spreadsheet/graph package. Molar ellipticity $\Delta\varepsilon$ (M^{-1} cm^{-1}) spectra were obtained through conversion of the direct CD measurements (θ, in millidegrees), using the relationship $\Delta\varepsilon = \theta/(33000cl)$, where c is the molar concentration and l is the path length.

Received: May 27, 2014
Published: May 30, 2014

   dx.doi.org/10.1021/bi500643b | *Biochemistry* 2014, 53, 3934−3939

Titrations. All chemicals were purchased from Sigma-Aldrich at the highest purity available, and UHQ water was used throughout (resistivity of 10^{-18} Ω^{-1} cm^{-1}). Small aliquots of fresh aqueous solutions were used to add metal ions (Cu^{2+} as $CuCl_2{\cdot}2H_2O$) and glycine for titrations. Titrations were conducted at pH 7.4 in the presence of 20 mM ethylmorpholine buffer.

The extinction coefficient at 280 nm was used to determine the concentration of full-length PrP^C and fragments, calculated from the total sum of the extinction coefficients for the number of aromatic residues and disulfide bridges in the peptide: 5690 M^{-1} cm^{-1} multiplied by the number of Trp residues in the peptide plus 1280 M^{-1} cm^{-1} multiplied by the number of Tyr residues plus 120 M^{-1} cm^{-1} multiplied by the number of disulfide bonds. Precise concentrations of peptides that did not contain aromatic residues were obtained via Cu^{2+} titrations with saturation at 1:1. Typically, the lyophilized peptide contained a moisture content of 20%.

Electron Paramagnetic Resonance (EPR). EPR spectra were recorded at 10 K using a Bruker Elexsys E580 spectrometer at an X-band microwave frequency of 9.38 GHz, using a microwave power of 0.5 mW across a sweep width of 2000 G, centered at 3000 G with a modulation amplitude of 10 G. Single scans were recorded, and the baseline spectrum was subtracted. Samples were loaded into an EPR quartz tube with an outside diameter of 4 mm and an inside diameter of 3 mm. Samples were run in 50 mM temperature-independent pH buffer composed of 60% HEPES and 40% phosphate buffer,[22] at pH 7.5 or 10.

Affinity Measurements. Glycine, the competing Cu^{2+} chelator used in calculating the affinity of the Cu^{2+}–peptide complexes, forms a $Cu(Gly)_2$ complex when bound to Cu^{2+}. The individual affinities of each glycine binding must be taken into account. The apparent affinities (K_{a1} and K_{a2}) at pH 7.4 are 7.4×10^5 and 7.4×10^4 M^{-1}, respectively.[23]

The concentration of Gly required for equal molar equivalents of Cu^{2+} to be bound to both the peptide and glycine is used to determine the affinity of Cu^{2+} for the protein using eq 1. The "free" Cu^{2+} refers to the concentration of Cu^{2+} not bound to either glycine or PrP peptides. A worked example of the calculation is given as Supporting Information.

$$K_d = [Cu^{2+}{}_{free}] = \frac{[Cu^{2+}{}_{total}] - [Cu^{2+}{}_{bound\ to\ protein}]}{1 + K_{a1}[Gly_{free}] + K_{a1}K_{a2}([Gly_{free}]^2)} \quad (1)$$

where at 50% saturation

$$[Cu^{2+}{}_{bound\ to\ protein}] = [protein_{total}]/2$$

$$[Gly_{free}] = [Gly_{total\ at\ 50\%\ saturation}] - [Cu^{2+}{}_{bound\ to\ protein}]$$

RESULTS AND DISCUSSION

First, we used visible CD to probe binding of Cu^{2+} to a simple tripeptide from the N-terminus of human/mouse PrP^C, KKR (residues 23–25). The tripeptide MKK was also studied because methionine is present in recombinant constructs of full-length PrP^C, previously used by ourselves and others. In the presence of Cu^{2+} ions at pH 7.4, the Vis-CD spectra of these two different N-terminal sequences are essentially the same with a negative ellipticity at 540 nm, associated with the d–d electronic absorption band, and a positive band at 318 nm, as shown in Figure 1. Cu^{2+} binds to these N-terminal tripeptides with a 1:1 stoichiometry (see Figure S1 of the Supporting Information). EPR spectra of the paramagnetic Cu^{2+} complex of MKK and KKR indicate a square-planar (type II) coordination geometry with $A_{||}$ and $g_{||}$ values typical of four-nitrogen (4N) ligands at pH 10. This suggests the Cu^{2+} coordination involves the N-terminal amino group and the following amide main-chain nitrogens (Figure 2). At physiological pH, the axial, square-planar, EPR spectrum is retained but there is a clear shift in the $A_{||}$ and $g_{||}$ values to those more

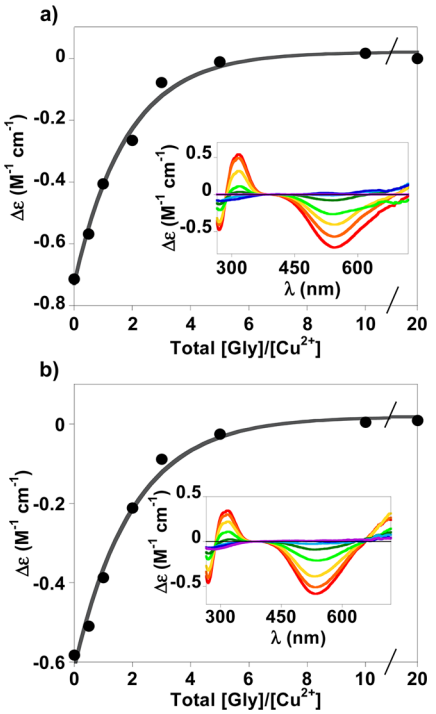

Figure 1. Visible CD and affinity of binding of Cu^{2+} to the N-terminus of PrP^C. Glycine competition binding curves taken at 540 nm for 200 μM Cu^{2+} bound to (a) 200 μM KKR and (b) 200 μM MKK at pH 7.4. Full spectra are inset for 0–20 molar equivalents glycine; the red trace is that without glycine and the purple trace that with 20 molar equiv of glycine. Calculated K_d values of 60 and 50 nM, respectively.

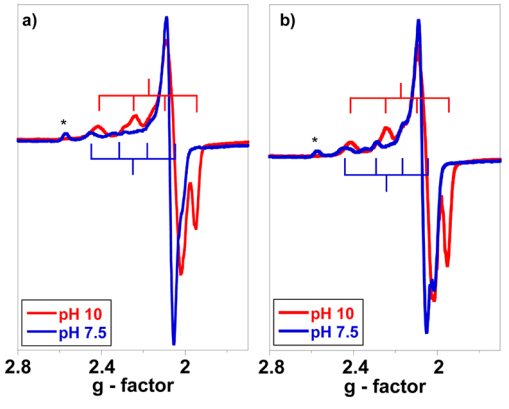

Figure 2. EPR spectra of Cu^{2+} complexed to the N-terminal amino group of PrP^C: (a) 200 μM KKR bound to 150 μM Cu^{2+} at pH 7.5 and 10 and (b) 200 μM MKK bound to 150 μM Cu^{2+} at pH 7.5 and 10. EPR spectra of the paramagnetic Cu^{2+} complex indicate a square-planar (type II) coordination geometry with $A_{||}$ and $g_{||}$ values typical of 4N ligands at pH 10. There is a clear shift in the $A_{||}$ and $g_{||}$ values at physiological pH more typical of a 3N1O or 2N2O complex at pH 7.5. An asterisk represents a contaminant.

dx.doi.org/10.1021/bi500643b | Biochemistry 2014, 53, 3934–3939

typical of nitrogen and oxygen ligands, a 3N1O or 2N2O complex, as highlighted in a Peisach and Blumberg plot[24] in Figure S2 of the Supporting Information. The pH dependence of the N-terminal complex is further probed by Vis-CD, as shown in Figure S3 of the Supporting Information.

The affinity of the N-terminal tripeptides complex at pH 7.4 was determined using glycine as a competing ligand, as shown in Figure 1. Nonchiral glycine has a known micromolar affinity for Cu^{2+},[23] and the resulting $Cu(Gly)_2$ complex is CD silent. Additions of increasing amounts of free glycine to the Cu–peptide complexes causes a reduction in the magnitudes of the CD bands at 540 and 318 nm. The concentration of glycine to cause a 50% reduction in the CD band intensity can be used to determine the apparent dissociation constant, K_d, at pH 7.4 (see Materials and Methods for details). It is clear from the binding curves that the affinity for the tripeptides is 60 nM for KKR and similarly 50 nM for MKK, compared to full-length PrP^C that has an affinity of ~20 nM for the first molar equivalent of Cu^{2+} binding to PrP^C.[14]

Table 1 compares the affinities of Cu^{2+} binding to recombinant full-length PrP^C and smaller recombinant and synthetic peptide fragments of PrP^C (previously determined[14]) to those of the model N-terminal tripeptides studied here. Previously, as many as 6 molar equiv of Cu^{2+} has been shown to bind PrP^C. The tight binding mode is thought to involve all four histidine residues from the octarepeat region (K_d of 20 nM or tighter[17,25]), along with two Cu^{2+} binding sites centered at His^{110} and His^{95} (K_d of ~20 nM) with a weaker affinity (K_d of 200 nM) for individual octarepeat binding sites.

Table 1. Comparison of Cu^{2+} Binding Affinities for Different Sites on PrP^C at pH 7.4

PrP fragment	K_d (nM)	PrP fragment	K_d (nM)
NH_3(KKR)[a]	61, 64	PrP(23–231 Δocta)[b]	19
NH_3(MKK)[a]	54, 40	hPrP(91–115 H96A)[b]	26
mPrP(23–231)[b]	20	mPrP(90–114)[b]	20
mPrP(57–67)[b] (single octarepeat)	200, 100[c]	mPrP(57–90)[b] (multiple octarepeats)	19[c]

[a]Determined from Vis-CD bands at 540 and 318 nm. [b]Adapted from ref 14. [c]Determined using tryptophan fluorescence instead of Vis-CD.

We were surprised that binding of copper to the individual octarepeats was weaker than binding of Cu^{2+} to the N-terminal amino group (K_d of 50–60 nM) as binding of Cu^{2+} to the N-terminal amino group has not previously been identified.[11,12] To support this observation, we performed a simple competition experiment between a single octarepeat and an N-terminal tripeptide. Figure 3 shows the Vis-CD spectrum of an equimolar mixture of MKK and a single octarepeat [PrP(58–68)] with increasing amounts of Cu^{2+}. It is clear that the Cu^{2+} ions load sequentially onto the MKK tripeptides first, as indicated by the initial appearance of a negative Vis-CD band at 540 nm. At 1 molar equiv of Cu^{2+} ions, a new set of Vis-CD bands appear, typical for the very different Vis-CD signals observed for binding of Cu^{2+} to a single octarepeat. This sequential loading is highlighted by difference spectra shown in panels c and d of Figure 3. These data strongly support the affinity measurements (Figure 1 and Table 1) indicating that for these model peptide fragments, Cu^{2+} preferentially binds to the N-terminal amino group before the single octarepeats.

Next we performed a similar competition experiment with the intact four-octarepeat peptide, PrP(58–91), shown in Figure 4. The spectra are dominated by the more intense CD bands for the individual octarepeats (Figure 4a). However, it is clear from the plot of the normalized intensity of the CD signal (Figure 4b) that the Cu^{2+} loads onto MKK (480 nm signal) before the individual octarepeats (CD bands at 580 and 670 nm). The MKK band saturates at ~2 molar equiv because Cu^{2+} ions also form the tighter affinity tetrahistidine complex, which is Vis-CD silent. The bands at 580 and 670 nm, typical of Cu^{2+} ions binding to a single octarepeat, saturate at ~5 molar equiv as one Cu^{2+} ion binds each of the four octarepeats.

The wavelength of the Vis-CD signal for the N-terminal amino group binding in these competition experiments does not precisely match the CD spectra for the MKK tripeptide alone with a negative peak centered at 540 nm. This is because the single octarepeats have a positive CD signal at wavelengths above 540 nm, which has the effect of canceling out the negative N-terminal CD signal to the longer wavelengths and so shifts the negative CD band to shorter wavelengths (~480 nm). This effect is apparent in Figures 3a, 4a, and 5b and also the simulated data in Figure 5d.

Finally, we wanted to determine if there was evidence of binding of Cu^{2+} to the N-terminal amino group preferentially over the individual octarepeats within full-length PrP^C(23–231). Figure 5 shows Vis-CD spectra of Cu^{2+} binding full-length mouse PrP^C(23–231) adapted from data we have

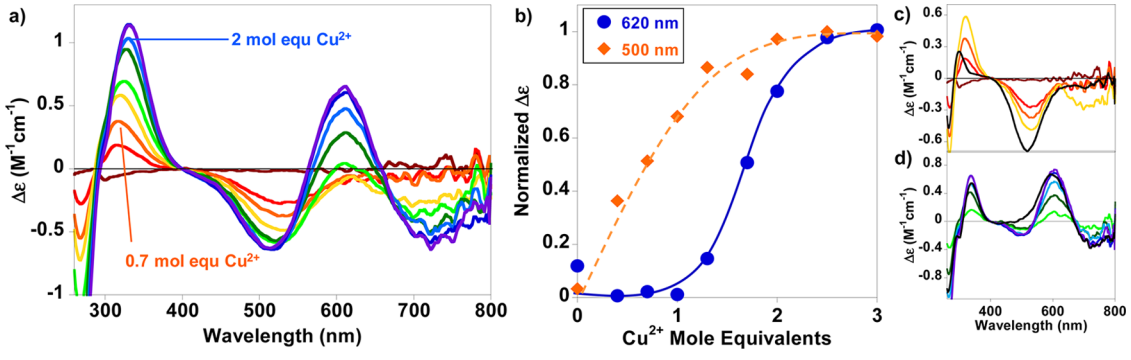

Figure 3. Visible CD competition of Cu^{2+} for MKK and an individual octarepeat. (a) MKK (100 μM) and single octarepeat (100 μM) with Cu^{2+} in 30 μM steps at pH 7.4 (red to purple). (b) Normalized intensity of the bands at 620 and 500 nm with an increasing level of Cu^{2+}. (c) Data presented in panel a for 0–1 molar equiv of Cu^{2+} (red to yellow) and 1 molar equiv of Cu^{2+} bound to MKK (black). (d) Data presented in panel a for the following two equivalents with the spectrum from the first equivalent subtracted (light green to purple) and 1 molar equiv of Cu^{2+} bound to a single octarepeat (black). Cu^{2+} preferentially binds to MKK over the single octarepeats.

dx.doi.org/10.1021/bi500643b | Biochemistry 2014, 53, 3934–3939

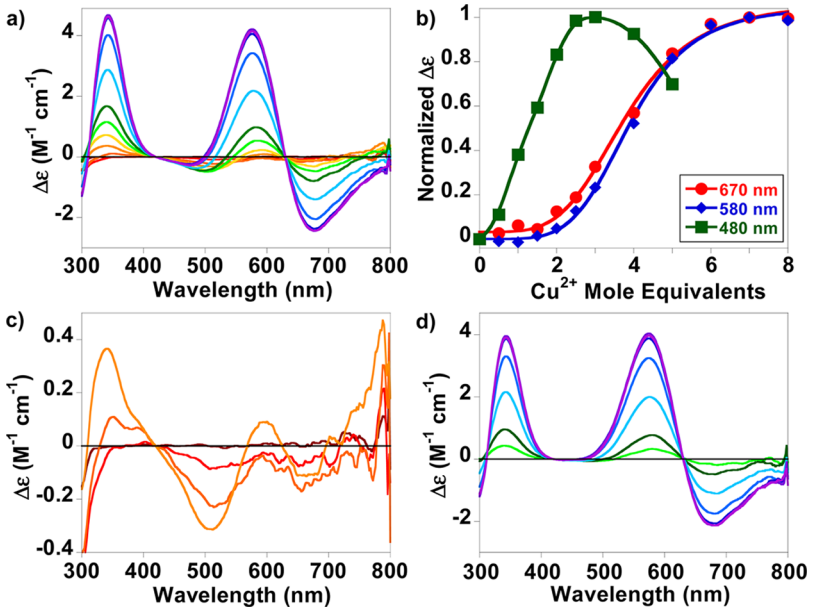

Figure 4. Visible CD competition of Cu^{2+} for MKK and PrP(58−91). (a) MKK (100 μM) and PrP(58−91) (100 μM) with Cu^{2+} in 50 μM steps at pH 7.4 (red to purple). (b) Normalized intensity of the bands at 480, 580, and 670 nm with an increasing level of Cu^{2+}. (c) Data presented in panel a for 0−1.5 molar equiv of Cu^{2+} (red to orange), highlighting the MKK contribution. (d) Difference spectra of the data presented in panel a for 2.5−8 molar equiv of Cu^{2+} (light green to purple), with the spectrum from the second equivalent subtracted from the subsequent spectra. The signal from MKK is not observed in the difference spectra.

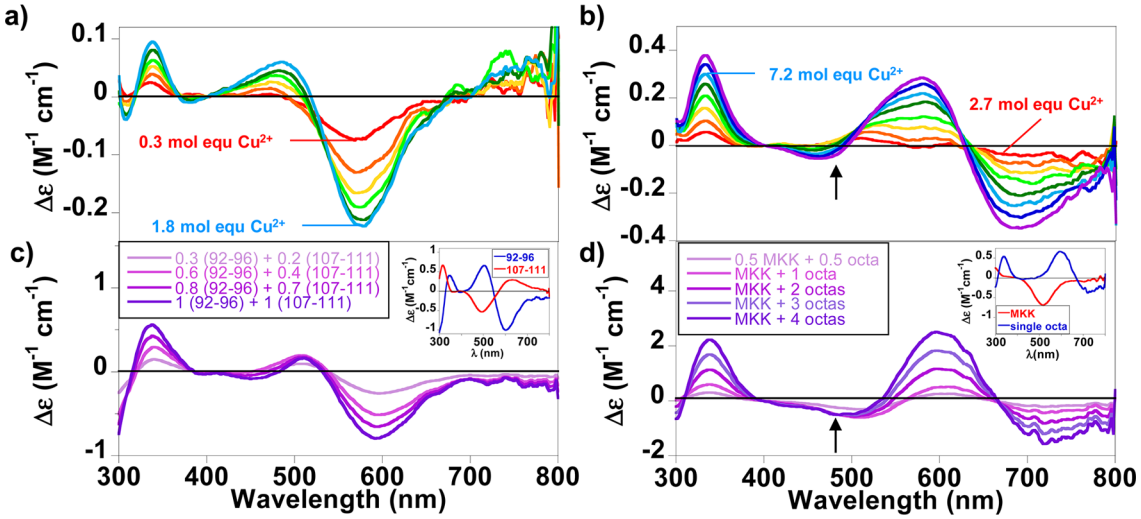

Figure 5. Visible CD of Cu^{2+} bound to full-length PrP^{C}(23−231). (a) Titration of Cu^{2+} into PrP(23−231) in 0.3−2 molar equiv. (b) Cu^{2+} (2−9 molar equiv) bound to PrP(23−231) with the first 2 molar equiv subtracted. (c) Simulated Vis-CD spectra of the titration of the first 2 molar equiv of Cu^{2+} into PrP(23−231) from individual spectra of PrP(107−111) and PrP(92−96) (inset). (d) Simulated Vis-CD spectra of the subsequent titration of Cu^{2+} into PrP(23−231) after the first 2 molar equiv from individual spectra of MKK plus four single octarepeats (inset). The arrow indicates the signal assigned to binding at the N-terminal amino group; there is a shift from 540 nm for the MKK signal to 480 nm because of overlap with the octarepeat signal. Panels (a) and (b) are taken from data previously published.[13]

previously published.[13] The general appearance of the series of spectra is rather complicated because of the multiple binding modes of Cu^{2+}, as shown in Figure S4 of the Supporting Information. However, when the spectrum after the addition of the first 2 molar equiv of Cu^{2+} (Figure 5a) is subtracted from subsequent spectra (Figure 5b), a clearer picture of Cu^{2+} binding sites sequentially loading onto PrP^{C} is apparent. In previous studies, the significance of the relatively weak negative CD band centered at ∼470 nm was overlooked. When these data are revisited, it is clear that this Vis-CD band is due to Cu^{2+} binding at the N-terminal amino group. Panels c and d of Figure 5 show how binding of Cu^{2+} to individual sites using small peptide fragments contributes almost precisely to the appearance of the Vis-CD spectrum for the full-length protein, with Cu^{2+} binding centered at His^{95} and His^{110} (Figure 5a,c) followed by binding at the N-terminal amino group and individual octarepeats (Figure 5b,d). Note that the tighter binding for the multiple octarepeats (K_d of 20 nM) is not observed in Vis-CD as it does not give a signal because there is no coordination to the chiral main chain. The sequential loading agrees with the affinities calculated (listed in Table 1). In full-length PrP^{C}(23−231), it is clear that binding at the N-

dx.doi.org/10.1021/bi500643b | Biochemistry 2014, 53, 3934−3939

terminal amino group has an affinity similar to or tighter than that of binding at the individual octarepeats.

Biological Significance. PrP^C is responsible for generating a range of TSEs in humans, cattle, and sheep and is linked with Cu^{2+} ion imbalance.[6] The presence of Cu^{2+} is associated with scrapie prion isolates and strains of prion disease,[7] and Cu^{2+} destabilizes the native fold of PrP^C.[26] Furthermore, Cu^{2+} binds to PrP^C *in vivo* at the synapse[3] and can trigger PrP^C endocytosis.[4] The concentration of Cu^{2+} can reach 15−250 μM at the synapse after neuronal depolarization;[3,27] consequently, nanomolar affinity is tight enough for binding to occur *in vivo*. The modes of binding of Cu^{2+} to PrP^C via multiple histidines, rather than individual histidines within the octarepeats,[17,25] or within the amyloidogenic region (His^{95} and His^{110}) have a considerably tighter affinity than the N-terminal amino group. The binding of Cu^{2+} at the N-terminal amino group of PrP^C is not a novel coordination mode as most proteins could bind Cu^{2+} in this way with similar ∼60 nM affinities. The principal Cu^{2+} binding site of Aβ and αSyn involve the N-terminal amino group but with a 1000-fold tighter affinity, with K_d values of 50 pM[20] and 200 pM,[28] respectively. These tighter affinities are due to the additional involvement of side-chain coordination. This raises the question of whether *in vivo*, loading of Cu^{2+} to the relatively weak individual octarepeat binding sites is physiologically significant. However, PrP^C is marked by its well-conserved natively unstructured domain of ∼100 residues that is capable of binding multiple Cu^{2+} ions. The transient high occupancy of these binding sites should not be ruled out during fluxes of Cu^{2+} ions in the microenvironment of the synaptic cleft.

■ ASSOCIATED CONTENT

Ⓢ Supporting Information

Detailed affinity calculations, Cu^{2+} coordination, and pH dependence of KKR and MKK complexes. This material is available free of charge via the Internet at http://pubs.acs.org.

■ AUTHOR INFORMATION

Corresponding Author

*E-mail: j.viles@qmul.ac.uk. Telephone: (44) 020 7882 8443. Fax: (44) 020 8983 0973.

Funding

This work was supported by a BBSRC Quota studentship (Biotechnology and Biological Sciences Research Council).

Notes

The authors declare no competing financial interest.

■ ACKNOWLEDGMENTS

Many thanks to Dr. Ray Burton-Smith and the Queen Mary EPR facility for help with EPR data acquisition.

■ ABBREVIATIONS

Aβ, amyloid-β; αSyn, α-synuclein; PrP^C, cellular prion protein; TSE, transmissible spongiform encephalopathy; Vis-CD, visible circular dichroism.

■ REFERENCES

(1) Viles, J. H. (2012) Metal ions and amyloid fiber formation in neurodegenerative diseases. Copper, Zinc and Iron in Alzheimer's, Parkinson's and Prion disease. *Coord. Chem. Rev. 256*, 2271−2284.

(2) Gaggelli, E., Kozlowski, H., Valensin, D., and Valensin, G. (2006) Copper homeostasis and neurodegenerative disorders (Alzheimer's, prion, and Parkinson's diseases and amyotrophic lateral sclerosis). *Chem. Rev. 106*, 1995−2044.

(3) Brown, D. R., Qin, K., Herms, J. W., Madlung, A., Manson, J., Strome, R., Fraser, P. E., Kruck, T., von Bohlen, A., Schulz-Schaeffer, W., Giese, A., Westaway, D., and Kretzschmar, H. (1997) The cellular prion protein binds copper in vivo. *Nature 390*, 684−687.

(4) Perera, W. S. S., and Hooper, N. M. (2001) Ablation of the metal ion-induced endocytosis of the prion protein by disease-associated mutation of the octarepeat region. *Curr. Biol. 11*, 519−523.

(5) Watt, N. T., Taylor, D. R., Kerrigan, T. L., Griffiths, H. H., Rushworth, J. V., Whitehouse, I. J., and Hooper, N. M. (2012) Prion protein facilitates uptake of zinc into neuronal cells. *Nat. Commun. 3*, 1134.

(6) Siggs, O. M., Cruite, J. T., Du, X., Rutschmann, S., Masliah, E., Beutler, B., and Oldstone, M. B. (2012) Disruption of copper homeostasis due to a mutation of Atp7a delays the onset of prion disease. *Proc. Natl. Acad. Sci. U.S.A. 109*, 13733−13738.

(7) Wadsworth, J. D., Hill, A. F., Joiner, S., Jackson, G. S., Clarke, A. R., and Collinge, J. (1999) Strain-specific prion-protein conformation determined by metal ions. *Nat. Cell Biol. 1*, 55−59.

(8) Sigurdsson, E. M., Brown, D. R., Alim, M. A., Scholtzova, H., Carp, R., Meeker, H. C., Prelli, F., Frangione, B., and Wisniewski, T. (2003) Copper chelation delays the onset of prion disease. *J. Biol. Chem. 278*, 46199−46202.

(9) You, H., Tsutsui, S., Hameed, S., Kannanayakal, T. J., Chen, L., Xia, P., Engbers, J. D. T., Lipton, S. A., Stys, P. K., and Zamponi, G. W. (2012) Aβ neurotoxicity depends on interactions between copper ions, prion protein, and N-methyl-D-aspartate receptors. *Proc. Natl. Acad. Sci. U.S.A. 109*, 1737−1742.

(10) Younan, N. D., Sarell, C. J., Davies, P., Brown, D. R., and Viles, J. H. (2013) The cellular prion protein traps Alzheimer's Aβ in an oligomeric form and disassembles amyloid fibers. *FASEB J. 27*, 1847−1858.

(11) Millhauser, G. L. (2004) Copper Binding in the Prion Protein. *Acc. Chem. Res. 37*, 79−85.

(12) Viles, J. H., Klewpatinond, M., and Nadal, R. C. (2008) Copper and the structural biology of the prion protein. *Biochem. Soc. Trans. 36*, 1288−1292.

(13) Klewpatinond, M., Davies, P., Bowen, S., Brown, D. R., and Viles, J. H. (2008) Deconvoluting the Cu^{2+} Binding Modes of Full-length Prion Protein. *J. Biol. Chem. 283*, 1870−1881.

(14) Nadal, R. C., Davies, P., Brown, D. R., and Viles, J. H. (2009) Evaluation of $Copper^{2+}$ Affinities for the Prion Protein. *Biochemistry 48*, 8929−8931.

(15) Ösz, K., Nagy, Z., Pappalardo, G., Di Natale, G., Sanna, D., Micera, G., Rizzarelli, E., and Sóvágó, I. (2007) Copper(II) Interaction with Prion Peptide Fragments Encompassing Histidine Residues Within and Outside the Octarepeat Domain: Speciation, Stability Constants and Binding Details. *Chem.—Eur. J. 13*, 7129−7143.

(16) Viles, J. H., Cohen, F. E., Prusiner, S. B., Goodin, D. B., Wright, P. E., and Dyson, H. J. (1999) Copper binding to the prion protein: Structural implications of four identical cooperative binding sites. *Proc. Natl. Acad. Sci. U.S.A. 96*, 2042−2047.

(17) Wells, M. A., Jelinska, C., Hosszu, L. L. P., Craven, C. J., Clarke, A. R., Collinge, J., Waltho, J. P., and Jackson, G. S. (2006) Multiple forms of copper(II) co-ordination occur throughout the disordered N-terminal region of the prion protein at pH 7.4. *Biochem. J. 400*, 501−510.

(18) Aronoff-Spencer, E., Burns, C. S., Avdievich, N. I., Gerfen, G. J., Peisach, J., Antholine, W. E., Ball, H. L., Cohen, F. E., Prusiner, S. B., and Millhauser, G. L. (2000) Identification of the Cu^{2+} binding sites in the N-terminal domain of the prion protein by EPR and CD spectroscopy. *Biochemistry 39*, 13760−13771.

(19) Binolfi, A., Quintanar, L., Bertoncini, C. W., Griesinger, C., and Fernández, C. O. (2012) Bioinorganic chemistry of copper coordination to α-synuclein: Relevance to Parkinson's disease. *Coord. Chem. Rev. 256*, 2188−2201.

(20) Sarell, C. J., Syme, C. D., Rigby, S. E., and Viles, J. H. (2009) Copper(II) binding to amyloid-β fibrils of Alzheimer's disease reveals a

picomolar affinity: Stoichiometry and coordination geometry are independent of Aβ oligomeric form. *Biochemistry 48*, 4388−4402.
(21) Jones, C. E., Abdelraheim, S. R., Brown, D. R., and Viles, J. H. (2004) Preferential Cu^{2+} Coordination by His96 and His111 Induces β-Sheet Formation in the Unstructured Amyloidogenic Region of the Prion Protein. *J. Biol. Chem. 279*, 32018−32027.
(22) Sieracki, N., Hwang, H., Lee, M., Garner, D., and Lu, Y. (2008) A temperature independent pH (TIP) buffer for biomedical biophysical applications at low temperatures. *Chem. Commun.*, 823−825.
(23) Dawson, R., Elliott, D., Elliott, W., and Jones, K. (1986) *Data for Biochemical Research*, 3rd ed., Clarendon Press, Oxford, U.K.
(24) Peisach, J., and Blumberg, W. (1974) Structural implications derived from the analysis of electron paramagnetic resonance spectra of natural and artificial copper proteins. *Arch. Biochem. Biophys. 165*, 691−708.
(25) Walter, E. D., Chattopadhyay, M., and Millhauser, G. L. (2006) The Affinity of Copper Binding to the Prion Protein Octarepeat Domain: Evidence for Negative Cooperativity. *Biochemistry 45*, 13083−13092.
(26) Younan, N. D., Nadal, R. C., Davies, P., Brown, D. R., and Viles, J. H. (2012) Methionine Oxidation Perturbs the Structural Core of the Prion Protein and Suggests a Generic Misfolding Pathway. *J. Biol. Chem. 287*, 28263−28275.
(27) Kardos, J., Kovács, I., Hajós, F., Kálmán, M., and Simonyi, M. (1989) Nerve endings from rat brain tissue release copper upon depolarization. A possible role in regulating neuronal excitability. *Neurosci. Lett. 103*, 139−144.
(28) Hong, L., and Simon, J. D. (2009) Binding of Cu(II) to Human α-Synucleins: Comparison of Wild Type and the Point Mutations Associated with the Familial Parkinson's Disease. *J. Phys. Chem. B 113*, 9551−9561.